



Initial Investigation of Wave Interactions During Simultaneous Valve Closures in Hydraulic Piping Systems

Kamil Urbanowicz¹ · Igor Haluch¹ · Anton Bergant² · Adam Deptuła³ · Paweł Śliwiński⁴

Received: 7 June 2023 / Accepted: 30 August 2023 / Published online: 26 September 2023
© The Author(s) 2023

Abstract

The effects of interference of pressure waves in simple piping systems were studied. A free-ware computer code Allievi developed at the University of Valencia was used to simulate dynamic waveforms in simple and complex networks. The tests were carried out according to three scenarios. No pressure increases significantly exceeding the Joukowski pressure in simple cases were noticed. When the effects of the simultaneous closing of three valves located at the three pressure reservoirs with pipes of the same diameter connected at "Y" junction were tested, it was shown that wave interference (between primary and reflected waves) is influenced strongly by the length of the analyzed pipes. Additionally, when a change of diameter was assumed at the "Y" junction, secondary waves appear, which are responsible for increased pressure in this type of the system (even when the lengths of the lines are identical). Water supply pipe systems are subject to cyclical loads and wave interference of similar types even during standard operations, that's why the understanding of this issue is crucial to effectively protect the systems from the risk of possible cracks, bursts, and leaks.

Keywords Water hammer · Three-reservoir-pipe problem · Method of characteristics · Wave interaction · Hydraulic systems

1 Introduction

This paper deals with an important practical problem that arises during rapid changes in fluid flow velocity in hydraulic, water supply, heating systems, and similar setups. In these systems, the flow is pressure-driven, meaning that there should be a pressure difference between the intake and outtake of a conduit for flow to occur. In real systems, during startup or shutdown (either due to accidental power failure, planned valve closure, pump speed changes, flow redirection through distributors, etc.), wave phenomena occur, which are responsible for sudden pressure and flow velocity variations at different sections of the piping system (Wylie et al. 1993). Numerical analysis is one way to safeguard these systems and identify the most heavily loaded components.

From the literature review, it is evident that water hammer in individual pipes during the closure of a single valve has been extensively studied in the past. However, the phenomenon of closing two valves and the interference generated by the resulting two pressure waves has only recently started to be analyzed (Bergant et al. 2021; Wang et al. 2019; Karadžić et al. 2018). Today much attention is given to the topic of slow valve closure (Yuce and Omer 2019; Han et al. 2022; Kodura 2016) as this method protects the systems from the adverse effects of water hammer. Zhang (2016) conducted research on this topic in a system equipped with a pump and a spherical valve, both of which were simultaneously closed to prevent large pressures. In recent papers, Bostan et al. (2021) improved the MOC method by combining implicit discretization with a time-variant estimation of friction losses. For multi-branched pipeline systems, an improved impedance method was proposed by Kim (2023). This promising solution can be used for laminar and turbulent flows. Zhang et al. (2023) proposed an efficient wave-tracking method (based on combined Lagrangian and Eulerian schemes), which has the same calculation accuracy as MOC but is 90% more efficient. Caponni et al. (2023) discussed and presented an innovative procedure for checking the in-line valve sealing in long, large-diameter transmission mains.

The cyclical appearance of increased pressures may occur in water supply systems (WSS) as a result of standard operation procedures (the result of opening and closing valves at end users, during maintenance procedures, etc.). The understanding of the mechanisms related to the superposition of multiple pressure waves is still not fully understood (Sun et al. 2017). Wave interference effects can cause dangerous pipe cracks, bursts, or even leakages. The objective of this paper is to deepen the understanding of wave interference effects in pipelines during transient events (valve closures).

This work focuses on analyzing three distinct scenarios related to power failure (closure of single valve and simultaneous closure of multiple valves) in hypothetical pipe systems (simple and branched). The most interesting case is a three-reservoir-piping system with valves located at the reservoirs and pipes connected through the “Y” junction. The effect of a sudden simultaneous closure of all three valves was not tested before (to the best knowledge of the authors). The generated pressure waves that interfere with exceeding Joukowsky pressure will be discussed in detail. Selection of such a hypothetical test stand can be used to test newly developed analytical solutions and CFD codes.

The primary objective of this paper is to show that even in very simple systems the wave interaction can be responsible for large water hammer pressures that can be dangerous for the pipe system elements (pipe, valve). Therefore, at the design stage of these systems, transient flow analyses of multiple valve closures should be performed to better understand and prevent large dynamic loads on the structural elements of the system, including pressure pipes and valves. The secondary objective is to test a freeware code (availability and capability) that is very popular among practitioners as well as scientists (Lončar et al. 2019; Lupa et al. 2022).

2 Choice of Research Software and a Brief Discussion of the Mathematical Model

In conducting the research outlined in this work, one of the publicly available computer codes designed for hydraulic transient flow analysis in pressure conduits will be utilized. In this way the reader can directly replicate the results of simulations presented in this paper. Among freeware programs (WHAMO – US Army Corps of Engineers; TSNNet – University

of Texas at Austin; Hytran – University of Auckland etc.), the Allievi code developed at the Polytechnic of Valencia (Allievi Homepage [n.d.](#)) was selected due to its modular structure and due its previous application in other scientific research studies (Lončar et al. 2019; Lupa et al. 2022). The Allievi code enables steady and unsteady flow simulations in pressurized pipes and open channels. In the code Quick Access toolbar (Fig. 1a–d) one can define: hydraulic system elements such as pumps, pipes, valves, tanks, protection devices, etc. (Fig. 1a); options to facilitate the creation of geometry and visualization of the design (Fig. 1b); define steady and unsteady flow parameters plus create graphs (Fig. 1c); change the language, upgrade the license or access the comprehensive manual in the form of a PDF file (Fig. 1d). Figure 1e shows an example of two sub-windows that can be accessed from the bar shown in Fig. 1c (on the left is Project Options, and on the right is the Wizard of Results window). The settings of the designed system (Fig. 1f for tanks; Fig. 1g for pipes; Fig. 1h for valves) can be modified in the options accessed from the Bottom windows.



Fig. 1 Options of Allievi software

Research on branched hydraulic systems of the "Y" junction type has been conducted so far in transmission systems (Taieb et al. 2020; Ramoul et al. 2017), characterized by long pipe lengths, as well as in laboratory setups with very short pipes (maximum length of 8 m) (Liao and Li 2010). Attempts have also been made to analytically solve this problem for unsteady pipe flow (Tijsseling and Bergant 2012). However, none of the aforementioned studies analyzed the simultaneous closure of three valves. Such a situation can occur in hydraulic systems due to power failure. The potential damages that an operator of such a system may face have been discussed in previous work (Bergant et al. 2010).

The equations that describe unsteady flow are the continuity equation and the equation of motion (Wylie et al. 1993):

$$\begin{cases} \frac{\partial p}{\partial t} + \rho c^2 \frac{\partial v}{\partial x} = 0 \\ \frac{\partial p}{\partial x} + \rho \frac{\partial v}{\partial t} + \rho g \sin \alpha + \frac{2}{R} \tau = 0 \end{cases} \quad (1)$$

where: c – the effective pressure wave propagation speed taking into account the deformation of the conduit (smaller than the speed of sound in an infinite fluid field) [m/s], p – pressure [Pa], t – time [s], v – bulk velocity [m/s], ρ – fluid density [kg/m^3], τ – wall shear stress [Pa], g – standard acceleration due to gravity [m/s^2], R – pipe inner radius [m], x – axial coordinate [m], α – angle of inclination of the pipe to the horizontal. Pressure $p(x,t)$ and flow velocity $v(x,t)$ are functions of independent variables x and t .

In *Allievi* software the wall shear stress is calculated in a quasi-steady manner:

$$\tau = f \frac{\rho v |v|}{8} \quad (2)$$

where: f – Darcy-Weisbach friction factor [-].

This is a simplified approach because the actual friction is the sum of a quasi-steady and frequency-dependent friction (modeled with a convolution integral) (Urbanowicz et al. 2023). Thus, the analyzed interactions between pressure waves may be modeled with (Eq. 2) more intense (increased/decreased peak/minimum values). Practitioners explain that the approach based on quasi-steady friction is sufficient because it can be used to predict critical the locations in the systems that are most exposed to high (pipe rupture) and low pressures (pipe collapse).

In *Allievi* software the method of characteristics MOC is used to transform a system of partial differential equations (Eq. 1) into two sets of characteristic ordinary differential equations:

$$C^+ : \begin{cases} \frac{dx}{dt} = +c \\ \frac{1}{c\rho} \frac{dp}{dt} + \frac{dv}{dt} + \frac{2}{\rho R} \tau = 0 \end{cases} \quad C^- : \begin{cases} \frac{dx}{dt} = -c \\ -\frac{1}{c\rho} \frac{dp}{dt} + \frac{dv}{dt} + \frac{2}{\rho R} \tau = 0 \end{cases} \quad (3)$$

which are numerically solved for given boundary conditions (Wylie et al. 1993). The numerical solution for internal pipe nodes that is based on the values from the previous time step at adjacent nodes is as follows:

$$\begin{cases} p_{t+\Delta t,i} = \frac{1}{2} \left[(p_{t,i-1} + p_{t,i+1}) + c\rho(v_{t,i-1} - v_{t,i+1}) + \frac{2c\Delta t}{R} (\tau_{t,i+1} - \tau_{t,i-1}) \right] \\ v_{t+\Delta t,i} = \frac{1}{2} \left[(v_{t,i-1} + v_{t,i+1}) + \frac{1}{c\rho} (p_{t,i-1} - p_{t,i+1}) - \frac{2\Delta t}{\rho R} (\tau_{t,i-1} + \tau_{t,i+1}) \right] \end{cases} \quad (4)$$

where: Δt – time step [s].



Work in the Allievi code begins with creating a scheme of the analyzed system (Fig. 2). The black dots in the scheme labeled N1, N2, etc. are the nodes where the pressure and flow velocity of the liquid are examined. The next step is to complete the following parameters about: pipe (for example length L [m] determining the distance between the valve 1 and valve 2 (System 2 in Fig. 2b), internal pipe diameter D [m], pipe wall thickness e [m] and pipe wall roughness ϵ [mm]), valve closing time and reservoirs. The pressure wave speed c is calculated by considering given diameter, wall thicknesses and liquid/pipe material coefficients. The last step is to customize the simulation parameters for steady and transient state calculations and to define other coefficients as gravity constants, type of fluid, Courant stability number, maximum numbers of iteration, etc.

3 Plan of Research Work

The research in this work was carried out for three distinct valve closure cases in pipe systems:

1. closing of a single valve in a reservoir-pipe-valve-reservoir system (Fig. 2a);
2. simultaneous closure of two valves in a reservoir-valve-pipe-pipe-valve-reservoir system (Fig. 2b);
3. simultaneous closure of three valves in a three-reservoir-system (Fig. 2c).

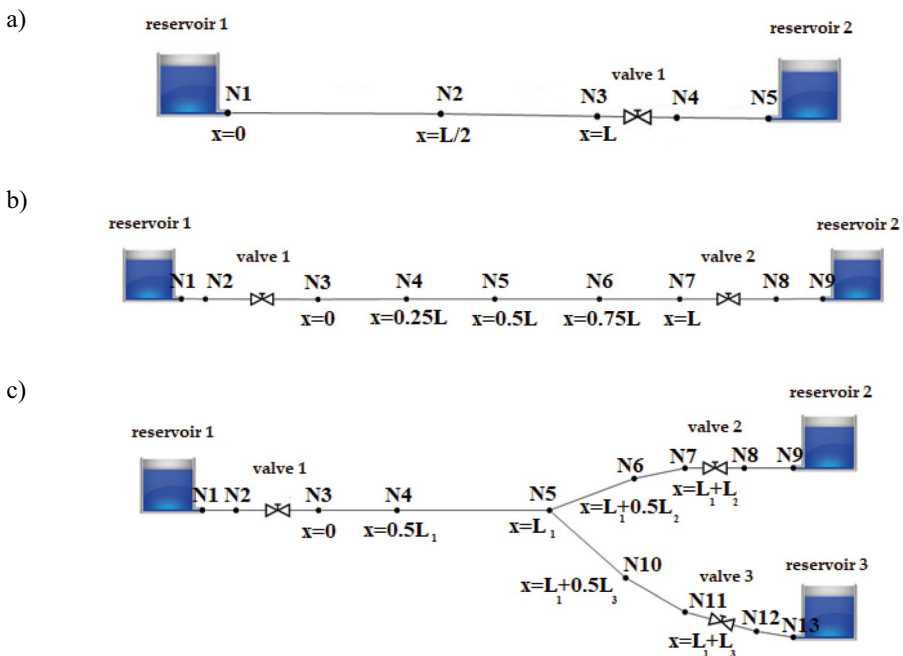


Fig. 2 Three distinct pipe systems used in numerical analysis



The selection of Systems 2 and 3 was specifically motivated by the objective to investigate the influence of mutual interference of pressure waves in multi-valve systems. Prior to transient state, it is assumed that there is a steady flow between the reservoirs.

3.1 Data for Single-Pipe Systems (Systems 1 and 2)

Since the only difference between single-pipe Systems 1 and 2 (Fig. 2a, b) is in the number of acting valves, all the investigations were carried out for the same input data. Separate studies were conducted for pipes made of steel and polyvinyl chloride (PVC) in both systems. The choice of pipe material in the Allievi software code only affects the pressure wave speed and does not provide an option to consider retarded strains that occur in real systems.

The influence of the working fluid (water, oil, and a water–oil mixture) on system response was examined as well. The choice of fluid (different viscosity, density, etc.) determined the assumed values of the dimensionless water hammer number (WHN) $Wh = (\nu L)/(cR^2)$ (Urbanowicz et al. 2023). A small value of WHN means that energy dissipation in the analyzed system with the flowing liquid will take relatively longer time. Assuming a zero value means that frictionless flow is analyzed, the pressure oscillations are periodic with non-decreasing amplitude. However, the assumption of a large value results in an increase in energy dissipation as a result of the increase of friction term. Practically all real systems represent the value of this number in the range $0 < Wh < 1$. WHN number can be represented as a ratio of Mach to Reynolds number multiplied by system scale factor: $Wh = (Ma/Re) \cdot (2L/R)$ explaining more intuitively why $Wh \ll 1$ in many practical applications.

To verify the Allievi code three values of WHN were selected: $Wh=0.0001$ (water flow WF), $Wh=0.001$ (water–oil mixture flow WOMF) and $Wh=0.01$ (oil flow OF). To fulfill these selected values of WHN the specific values of pipe diameters were assumed: $D=40$ mm (a typical household end user-pipes), $D=125$ mm and $D=300$ mm (used in distribution networks in commercial/industrial systems).

Additionally, the effects of three different flow regimes were tested, for three values of the Reynolds number: a) $Re=1000$ (laminar flow LF); b) $Re=3000$ (transitional flow TRF); c) $Re=10000$ (turbulent flow TUF). The pipe length and initial flow velocity were calculated using the transformed formulas of water hammer number and Reynolds number.

$$L = \frac{cR^2 Wh}{\nu} \quad (5)$$

$$v_0 = \frac{\nu Re}{D} \quad (6)$$

where: ν – kinematic viscosity [m^2/s].

All assumed and calculated values of parameters needed to perform simulations in single-pipe systems (Systems 1 and 2) are collected in Table 1.

In total 18 transient flow cases were investigated (9 in the metal pipe and 9 in the PVC pipe) for each valve closure case in pipe Systems 1 and 2.

In pipe Systems 1 and 2 the flow occurs from the upstream high-pressure reservoir UR located at $x=0$ of the systems in Fig. 2a, b to the downstream low-pressure reservoir DR (located at the $x=L$). To exclude the possibility of transient vaporous cavitation as it significantly modifies the nature of unsteady flow phenomena (water hammer equations are valid



Table 1 Values of boundary and initial parameters (for single-pipe Systems 1 and 2)

Calculated parameter	<i>WF</i>		<i>WOMF</i>		<i>OF</i>	
	<i>Wh</i> = 0.0001 <i>D</i> = 40 mm <i>v</i> = 0.0000011 m ² /s <i>ρ</i> = 1000 kg/m ³		<i>Wh</i> = 0.001 <i>D</i> = 125 mm <i>v</i> = 0.00001 m ² /s <i>ρ</i> = 940 kg/m ³		<i>Wh</i> = 0.01 <i>D</i> = 300 mm <i>v</i> = 0.0001 m ² /s <i>ρ</i> = 860 kg/m ³	
	<i>steel</i>	<i>PVC</i>	<i>steel</i>	<i>PVC</i>	<i>steel</i>	<i>PVC</i>
<i>L</i> [m]	50.11	18.98	498.84	120.93	2528.64	455.87
<i>c</i> [m/s]	1378	522	1277	310	1124	203
<i>v</i> ₀ (LF) [m/s]	0.0275		0.08		0.33	
<i>v</i> ₀ (TRF) [m/s]	0.0825		0.24		1.00	
<i>v</i> ₀ (TUF) [m/s]	0.275		0.80		3.33	
<i>p</i> _{UR} (LF) [Pa]	139255.7	115693.3	198125.2	124792.2	449265.7	164052.1
<i>p</i> _{UR} (TRF) [Pa]	215220.6	144468.3	394267.4	172338.4	1229636.3	304693.3
<i>p</i> _{UR} (TUF) [Pa]	481885.4	245468.3	1099577.1	343249.7	4579589.8	908061.1

only for the pure liquid flow (Wylie et al. 1993) it is assumed that the pressure at the downstream end of the system i.e., at the node located at the right-hand side valve (in System 1 – node N3; in System 2 – node N7), has a fixed value calculated from the following equation:

$$p_{DR} = p(L, 0) = p_a + \rho c |v_0| \tag{7}$$

From Eq. (7) it follows that the downstream pressure is assumed as a sum of atmospheric pressure and Joukowsky pressure rise (assumed positive). The upstream pressure is next calculated as:

$$p_{UR} = p(0, 0) = \Delta p + p(L, 0) = f \frac{\rho L v_0^2}{2D} + p_a + \rho c |v_0| \tag{8}$$

The Darcy-Weisbach friction factor is Reynolds number dependent (in turbulent flow also pipe wall roughness dependent) and in this work is calculated by using one of the following two formulas:

$$\left\{ \begin{array}{l} f = \frac{64}{Re} \quad \text{if } Re \leq 2320 \\ f = \frac{0.25}{\left[\log \left(\frac{\epsilon}{3.7D} + \frac{5.74}{Re^{0.9}} \right) \right]^2} \quad \text{if } Re > 2320 \end{array} \right. \tag{9}$$

Turbulent friction factor was calculated using Swamee and Jain (1972) approximation of the Colebrook-White equation, assuming the pipe’s effective roughness height: $\epsilon = 0.045$ mm for metal pipe and $\epsilon = 0.025$ mm for PVC pipe. All calculated upstream reservoir UR pressures are collected in Table 1.

In Allievi code the pressure head values *H* [m] were needed to set in all implemented reservoirs:

$$H = \frac{P}{\rho \cdot g} \tag{10}$$

In (Eq. 10) $p = p_{UR}$ for the “high-pressure” reservoir and $p = p_{DR}$ for the downstream “low-pressure” reservoir.

To wider analyze the damping ratio of pressure waves, that occur after the valve closure, the Damping Ratio Coefficient DRC is calculated for all analyzed cases in pipe Systems 1 and 2:

$$DRC = \frac{\sum_{i=1}^n \frac{p_{max_{i+1}}}{p_{max_i}}}{n} \quad (11)$$

where p_{max_i} and $p_{max_{i+1}}$ are the maximal pressures at the preceding and the following pressure amplitudes. In qualitative analysis results from the first seven amplitudes are analyzed, which means that $n = 6$.

3.2 Data for Three-Reservoir-Pipe System (System 3)

The steady flow between the three reservoirs (Fig. 2c) was investigated first. Determining the direction of the flow, whether it originates from one or multiple reservoirs, is not a trivial matter (Rangaraju and Sathuraman 1969; Haidera and Valentine 2018; Singh 1982; Loganathan and Kuo 1985). In this paper the water flow in steel pipe system is studied. Two sub-variants will be examined: 3.1) assuming a constant internal diameter of the pipes, $D = \text{const.}$, with variable pipe lengths, $L = \text{var.}$; and 3.2) assuming a constant initial Reynolds number, $Re_0 = \text{const.}$, with pipes of different diameters, $D = \text{var.}$, and variable pipe lengths, $L = \text{var.}$ In Sub-variant 3.1, the initial flow (pre-transient) was analyzed to be either laminar or turbulent. In Sub-variant 3.2, cases were investigated where steady flow was assumed to be laminar, transitional, or turbulent. It should be noted that we are interested in the flow from reservoir 1 to reservoirs 2 and 3, and the relationship between the pressures in the respective reservoirs in the steady flow preceding the water hammer event is described by the following dependencies:

$$\begin{cases} p_{R2} = p_{R1} - \Delta A \\ p_{R3} = p_{R1} - \Delta B \end{cases} \quad (12)$$

where pressure losses ΔA and ΔB are calculated taking into account the linear pressure drop in analyzed pipes:

$$\begin{cases} \Delta A = \frac{\rho}{2} \left[\frac{f_1 L_1 v_1^2}{D_1} + \frac{f_2 L_2 v_2^2}{D_2} \right] \\ \Delta B = \frac{\rho}{2} \left[\frac{f_1 L_1 v_1^2}{D_1} + \frac{f_3 L_3 v_3^2}{D_3} \right] \end{cases} \quad (13)$$

In case when $\Delta A > \Delta B$, the pressure in reservoir 2 was set to be:

$$p_{R2} = p_a + \rho c_{max} |v_{max}| \quad (14)$$

and next the pressure in the reservoir 1 $p_{R1} = p_{R2} + \Delta A$ and in reservoir 3 $p_{R3} = p_{R1} - \Delta B$ are calculated.

Otherwise, when $\Delta B > \Delta A$:

$$p_{R3} = p_a + \rho c_{max} |v_{max}| \quad (15)$$

and $p_{R1} = p_{R3} + \Delta B$, $p_{R2} = p_{R1} - \Delta A$.



In Sub-variant 3.2 (characterized by constant Reynolds numbers and different wave velocities c resulting from selected different pipe diameters), in cases where $L_1 \neq L_2 \neq L_3$, the distinct lengths of the pipes were selected to avoid the need for interpolation in numerical calculations satisfying the Computational Compliance Criteria CCC (Urbanowicz 2017). Fulfillment of CCC criteria guarantees proper numerical simulation compatibility because too coarse pipe division into computational reaches (pipeline discretized spatial sections) ($N < 10$) may cause errors in the numerical solution in the form of incorrect over/understated dissipation and changes of waves dispersion.

The number of computational reaches in the shortest pipe was set to $N = 20$. In the studies related to this Sub-variant, it was assumed that the shortest pipe is pipe 3, from the "Y" junction to the valve at the reservoir 3 (except in cases where the pipe lengths are equal).

The calculated values of pressures in the reservoirs (water column height in meters) and the initial velocities required to ensure assumed pre-transient flow in the pipes in Sub-variant 3.1 are presented in Table 2. In all simulations conducted in this sub-variant, a uniform internal diameter of 4 cm was assumed for the pipes, resulting in a wave velocity of $c = 1378.2$ m/s in the steel pipe. The following Reynolds numbers were assumed for the respective pipes in this sub-variant: a) in laminar flow case— $Re_1 = 2200$ in pipe L_1 ; $Re_2 = 1500$ in pipe L_2 ; and $Re_3 = 700$ in pipe L_3 ; b) in turbulent flow case— $Re_1 = 10000$ in pipe L_1 ; $Re_2 = 6000$ in pipe L_2 ; and $Re_3 = 4000$ in pipe L_3 .

Table 2 Data for three-reservoir-pipe system (System 3): Sub-variants 3.1 ($D = \text{const} = 4$ cm) and 3.2 ($Re = \text{const}$)

Test	Flow type	L_1 [m]	L_2 [m]	L_3 [m]	v_1 [m/s]	v_2 [m/s]	v_3 [m/s]	H_{R1} [m]	H_{R2} [m]	H_{R3} [m]
$D = \text{const} = 4$ cm										
3.1.1	laminar	50	50	50	0.0605	0.04125	0.01925	18.8397	18.8283	18.8308
3.1.2	laminar	50	35	25	0.0605	0.04125	0.01925	18.8383	18.8283	18.8305
3.1.3	laminar	50	30	15	0.0605	0.04125	0.01925	18.8379	18.8283	18.8304
3.1.4	laminar	50	15	5	0.0605	0.04125	0.01925	18.8365	18.8283	18.8295
3.1.5	turbulent	50	50	50	0.275	0.165	0.11	49.1779	48.9631	48.9948
3.1.6	turbulent	50	35	25	0.275	0.165	0.11	49.1592	48.9631	48.9914
3.1.7	turbulent	50	30	15	0.275	0.165	0.11	49.1530	48.9631	48.9913
3.1.8	turbulent	50	15	5	0.275	0.165	0.11	49.1343	48.9631	48.9788
$Re = \text{const}$										
3.2.1	laminar	50	50	50	0.01375	0.022	0.0366	15.5338	15.5324	15.5307
3.2.2	laminar	50	34.7	25	0.01375	0.022	0.0366	15.5324	15.5313	15.5307
3.2.3	laminar	50.3	30.1	15	0.01375	0.022	0.0366	15.5319	15.5309	15.5307
3.2.4	laminar	50	14.9	5	0.01375	0.022	0.0366	15.4315	15.4308	15.4308
3.2.5	transition	50	50	50	0.04125	0.066	0.11	25.9533	25.9450	25.9345
3.2.6	transition	50	34.7	25	0.04125	0.066	0.11	25.9450	25.9386	25.9345
3.2.7	transition	50.3	30.1	15	0.04125	0.066	0.11	25.9417	25.9358	25.9345
3.2.8	transition	50	14.9	5	0.04125	0.066	0.11	25.6390	25.6349	25.6350
3.2.9	turbulent	50	50	50	0.1375	0.22	0.366	62.5024	62.4345	62.3478
3.2.10	turbulent	50	34.7	25	0.1375	0.22	0.366	62.4346	62.3817	62.3478
3.2.11	turbulent	50.3	30.1	15	0.1375	0.22	0.366	62.4076	62.3591	62.3478
3.2.12	turbulent	50	14.9	5	0.1375	0.22	0.366	61.3829	61.3493	61.3502

The calculated input data for Sub-variant 3.2 (constant Reynolds number in all pipes) are also presented in Table 2. The assumptions for this case, not specified in the table, include different pipe diameters: $D_1 = 8$ cm in pipe L_1 ($c_1 = 1328$ m/s), $D_2 = 5$ cm in pipe L_2 ($c_2 = 1365$ m/s), and $D_3 = 3$ cm in pipe L_3 ($c_3 = 1392$ m/s). In this sub-variant, the following cases were examined for the initial Reynolds number: a) laminar flow case with $Re = 1000$; b) transitional flow case with $Re = 3000$; c) turbulent flow case with $Re = 10000$.

It should be noted that the Allievi code calculates the initial flow velocities in all pipes based solely on the specified pressures heads in the reservoirs.

3.3 Discussion about Simulation Results in Single-Pipe Systems 1 and 2

As the results of damped pressure pulsations for the classical case with instantaneous single valve closure in the pipe System 1 (Fig. 2a) are very similar, discussion will be focused on selected qualitative results. Exemplary results for turbulent flow case in the steel pipe System 1 (marked red in Table 1) are shown in Fig. 3a–c. It is clear that the pressure damping is very low – nearly not noticeable for the water flow case when $Wh = 0.0001$ (turbulent initial flow – Fig. 3a). In oil–water mixture flow where $Wh = 0.001$ (Fig. 3b) the damping that is modelled with Allievi program is more noticeable. As expected, the most significant pressure wave damping is observed in transient oil pipe flow, specifically when the value of Wh is 0.01 (as shown in Fig. 3c).

For all cases the maximal pressures and times of water hammer period (longer for larger values of water hammer number) differ. The quantitative results calculated at the valve section and at the middle pipe section are similar. Consequently, Table 3 in Appendix A collects the results at the valve only.

From quantitative analysis (Table 3), it can be observed that the damping increases with an increase in the water hammer number. Interestingly, slightly higher DRC values were obtained for the PVC pipe compared to the metal pipe in the case with $Wh = 0.01$. However, such a discrepancy is inconsistent with the knowledge of transient flows in plastic pipes. Water distribution systems made of plastic pipes exhibit an enhanced damping effect associated with the occurrence of retarded strain phenomena (Andrade et al. 2023; Pan et al. 2022).

In System 2 there are two valves installed: one at the upstream end section at the reservoir 1, and the other one at the downstream end section at the reservoir 2 (Fig. 2b). Simultaneous closure of the two valves produces two pressure waves. The wave of increased pressure occurred at the beginning of transient flow at the valve located downstream (node N7), while the wave of decreased pressure occurred at the valve located upstream (node N3). In order to compare the results with those obtained in the single-pipe System 1, turbulent flow case in the System 2 with a metal pipe is selected again.

From the comparison of the results in Fig. 3a–f it can be observed that in the System 2, the "line packing" phenomenon discussed in reference (Wylie et al. 1993) is not as significant as when a single valve is closed. The maximum pressures in System 2 were lower for the same initial conditions. This is evident in the case of $Wh = 0.001$ (Fig. 3e), where the maximum pressure at the first peak was approximately 225 m, while in System 1 (Fig. 3b), it was about 250 m. Similarly, for $Wh = 0.01$ (at the first peak, Fig. 3f) the pressure was approximately 830 m, whereas in the previous study (Fig. 3c), it was about 900 m.

Interesting results were obtained in the middle section of the single-pipe System 2, where the pressure remained unchanged. Its value remained constant, equal to the pressure before the occurrence of the water hammer event. This situation results from the



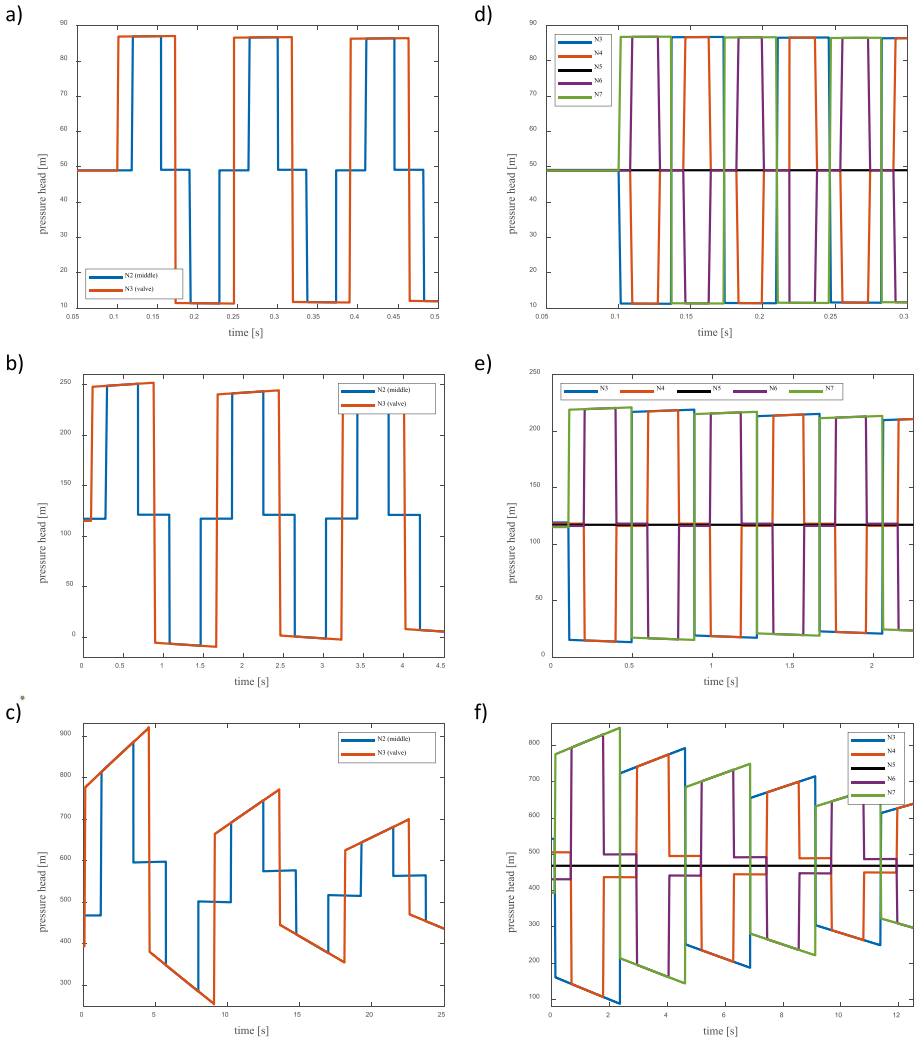


Fig. 3 Exemplary results for turbulent flow case in a single-steel pipe: **a, b, c** – System 1; **d, e, f** – System 2

simultaneous closure of the valves, causing the wave of increased pressure and the wave of decreased pressure to meet at this point in the uniform pipe. The interference of these two waves leads to the constant pressure at all times ($DRC = 1$).

Considering that in the analyzed case, two sections are significant, the quantitative analysis (Table 3) was performed for section N3 located at the valve 1, and section N7 located at the valve 2 (Fig. 2b). From Table 3 it follows that the damping ratio is very similar at the two analyzed cross sections of the tested system in the cases when Wh number is relatively small ($Wh \leq 0.001$). Only in the case of oil flow the damping is evidently larger at the upstream end section in comparison to the downstream end.

The simulations conducted clearly showed that the Allievi computer code is based on a simplified quasi-steady skin friction model and neglects the retarded strain taking place in plastic pipes. In this approach, wave reflections result in abrupt (linear) changes in pressure

histories. However, such pressure changes are not observed in practice. The waveforms are rounded, and apart from the dissipation phenomenon, dispersion of the waveforms occurs due to the influence of the frequency-dependent friction (Urbanowicz et al. 2023; Cao et al. 2022).

3.4 Discussion about Simulation Results in Three-Reservoir-Pipe System

Due to the complexity of transient flow in three-reservoir-pipe system (System 3 in Fig. 2c), numerical studies were conducted in a limited range. The tests were performed for WSS characterized by small diameters pipes. The simulations carried out for relatively low Reynolds numbers were intentional, because we are planning to construct an experimental apparatus and perform measurements. Due to the limited space at the university laboratory in Szczecin and safety reasons, the experimental research on full scale facility is not feasible. The System 3 is comprised of three reservoirs, and the pressure head differences between the reservoirs govern the flow between them. Valves are installed at the reservoir outlet(s)/inlet(s). In the event of a power failure, there is a high probability that all three valves will close simultaneously. This would generate three pressure waves that would propagate through the analyzed system, interacting with each other.

3.4.1 Constant Diameter of Pipes

The analysis is focused on two selected turbulent flow cases: a) all pipes with equal length: $L_1=L_2=L_3=50$ m (only discussed); b) the pipe lengths were set as follows: $L_1=50$ m, $L_2=15$ m, $L_3=5$ m (Fig. 4). The selected case for analysis is highlighted in green color and marked as bold in Table 2.

The conclusion from Test 3.1.5 (equal pipe lengths) is: the pressure at “Y” junction (N5) remains constant at steady flow value (similar as at the middle section in the single-pipe system 2 – Fig. 2d–f, when two valves were closed simultaneously); the maximum pressures do not exceed those observed in tests done for the System 1 (Fig. 2a–c).

The following conclusions can be drawn from tests carried out when the lengths of the pipes differ for Test 3.1.8 (Fig. 4): the pressure rises in all pipes (L_1, L_2, L_3) are significantly larger surpassing the Joukowski pressure rise; at the “Y” junction (N5), the pressure is not constant and pulsates in the opposite phase to the pressure changes in the L_1 pipe (nodes N3, N4); at the mid and far end sections of pipes L_2 (N6, N7) and L_3 (N10, N11) the pressure pulsations nearly overlap (same phase) with only slight differences observed in the peak and minimum values; despite attempts to increase the steady flow pressure cavitation phenomena occur in all pipes (however, not at the Y junction); in the next stage of our computational research longer time simulations should be performed to indicate if the phenomenon of resonance takes place; for more reliable analysis, the unsteady frictional resistance needs to be considered as well (in future research).

The previously used quantitative parameter *DRC* (Eq. 11) fails for the three-reservoir-pipe system because the pressure changes observed were chaotic and lacked clearly distinguishable amplitudes, making it difficult to programmatically determine the maximum values for a given impact period. A new dimensionless quantitative parameter named the Over Pressure Coefficient (*OPC*) (defined as the ratio of the actual to the theoretical pressure increase predicted by Joukowski’s formula) is introduced:



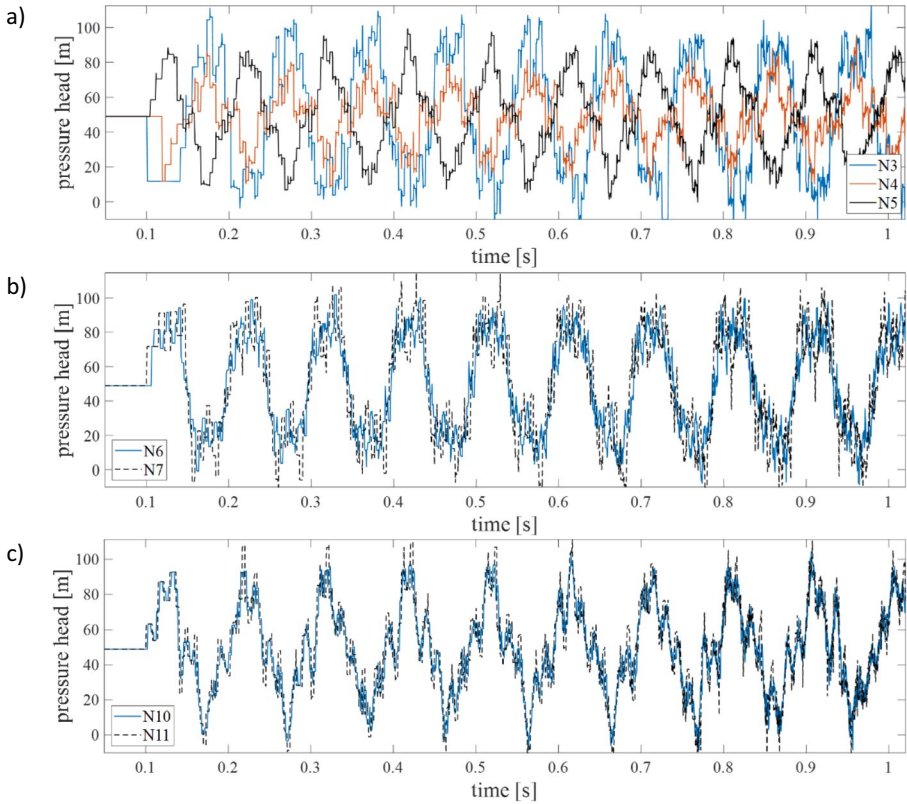


Fig. 4 Results for turbulent flow case in three-reservoir-pipe system (Test 3.1.8; $L_1=50$ m, $L_2=15$ m and $L_3=5$ m)

$$OPC = \frac{P_{max} - P_{initial}}{P_{max,J} - P_{initial}} = \frac{P_{max} - P_{initial}}{P_{initial} + \rho c |v_0| - P_{initial}} = \frac{P_{max} - P_{initial}}{\rho c |v_0|} \quad (16)$$

Calculated results of *OPC* are presented in Table 4 in Appendix A. Quantitative studies of *OPC* revealed that in systems based on pipes with constant diameters, significant pressure exceeding the values observed in the steady-state flow plus Joukowsky pressure rise can occur in certain pipe configurations. The quantitative parameter in the system where pipe L_3 had the shortest tested length (Test 3.1.4) reached a value as high as $OPC=5.73$. Conclusion: in systems based on pipes of different lengths, potentially dangerous situations similar to resonance can occur, and in several tests this flow behavior led to the appearance of transient cavitating areas. Both cavitation and significant pressure increases can contribute to the occurrence of potentially hazardous phenomena and, in some cases, even failures of pipe system components (Bergant et al. 2010).

In addition, qualitative and quantitative analysis of an extra Test 3.1.9 (Table 5), performed for a large-scale system with the ratios of pipe lengths (L_2/L_1 and L_3/L_1) as in Test 3.1.8, are presented in Appendix B. The results of Tests 3.1.8 and 3.1.9 exhibit a noticeable qualitative similarity of pressure-histories, which is confirmed by similar *OPC* values for both cases. This shows how important are the pipe length ratios in pipe networks.

3.4.2 Constant Reynolds Number

For the qualitative analysis in this subsection, the following cases of turbulent flow (highlighted in bold in Table 2) were selected: a) pipes with equal lengths $L_1 = L_2 = L_3 = 50$ m (Fig. 5); b) different pipe lengths ($L_1 = 50$ m, $L_2 = 34.7$ m, and $L_3 = 15$ m – Fig. 6).

In Fig. 5a, pulsations can be observed in three sections of the pipe L_1 . Numerical studies have revealed that in a system composed of pipes with different internal diameters, characteristic pressure peaks appear at the beginnings and ends of the pressure wave's crests and troughs at sections N3, N4 and N5 (at "Y" junction). Similar peaks to those observed at the N3 section (Fig. 5a) occurred in the case of fluid–structure interaction phenomena in pipelines (Andrade et al. 2022; Bayle and Plouraboué 2023). However, in our cases, these peaks are the result of liquid pressure wave interference. This situation starts with a single increase observed at $t \approx 0.137$ s, which then develops into a group of cyclically appearing peaks at section N5 ($t \approx 0.137$ s, $t \approx 0.21$ s, $t \approx 0.285$ s, $t \approx 0.36$ s,

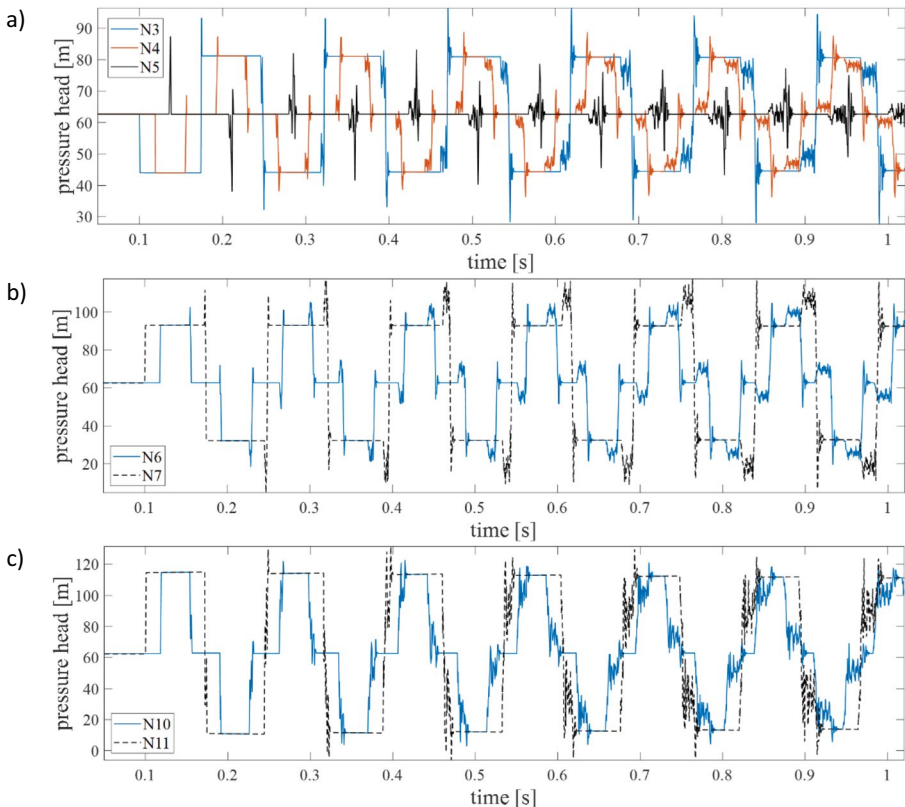


Fig. 5 Results for turbulent flow case in three-reservoir-pipe system (Test 3.2.9; $L = \text{const} = 50$ m)

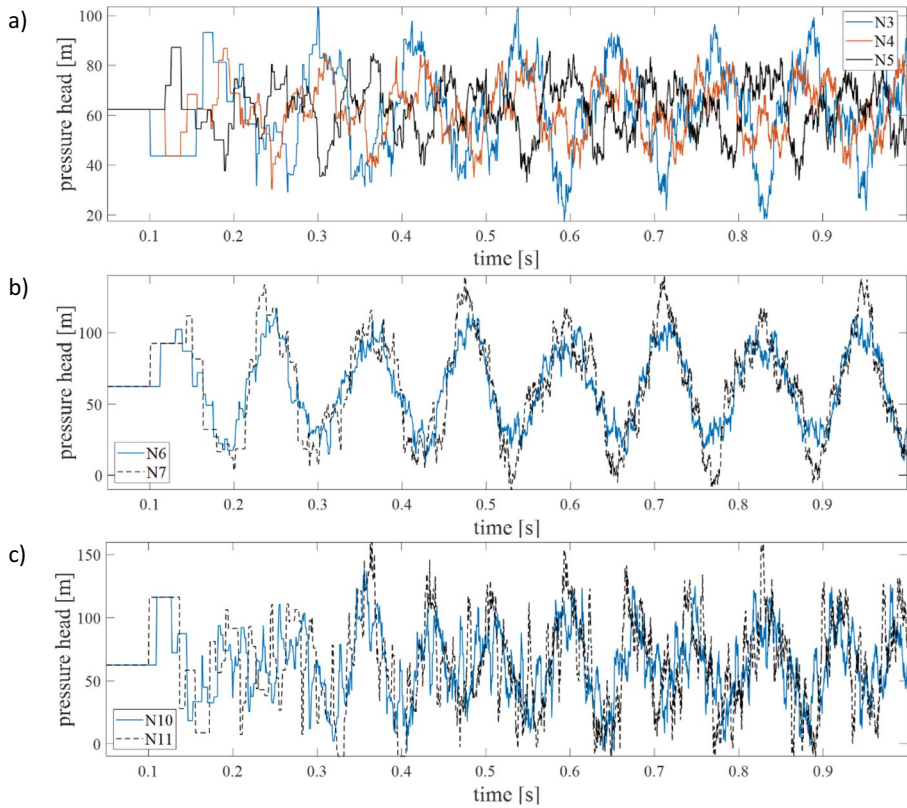


Fig. 6 Results for turbulent flow case in three-reservoir-pipe system (Test 3.2.10; $L_1=50$ m, $L_2=34.7$ m, $L_3=25$ m)

$t \approx 0.43$ s ...). Noticeable peaks are the result of pressure wave reflections at the "Y" junction, where the diameter changes. Similar peaks are noticeable in the other two pipes L_2 and L_3 of the System 3 (Fig. 5b, c), where the maximum pressure head values are approximately 120 m.

In Fig. 6, it can be seen, that when the lengths of pipes L_2 and L_3 differ, the situation is similar to the one observed previously for the case 3.1.8 shown in Fig. 4. In pipe L_1 , at junction N5, the pulsation occurs in the antiphase to the pulsations at junctions N3 and N4. The highest pressures are observed at the junction N11 (valve 3), where the pulsation intensifies during the first amplitude, thereby posing a greater threat to the pipes. The pressure increments at junctions N3 (Fig. 6a), N7 (Fig. 6b), and N11 (Fig. 6c) have values significantly higher than those estimated by the Joukowsky formula. In pipe L_2 (Fig. 6b), the pulsation waveforms in both analyzed sections are in the same phase.

The waveforms observed in pipe L_3 (Fig. 6c) are highly chaotic. In the initial period of the impact, typical pressure amplitudes are not observed at junctions N10 and N11 due to intense interference of primary and secondary waves generated in this shortest pipe. In addition, at N11 transient cavitating flow occurs (Fig. 6c at $t \approx 0.325$ s and $t \approx 0.4$ s).

From the obtained results of the quantitative analysis (Table 4), it can be seen, that in systems where the initial Reynolds number is constant in all pipes, the pressure increments, which can be expected, should not exceed the value of the *OPC* parameter: $OPC = 3$. It should be noted, that in systems that resemble real-world systems with variable diameters, the intensity of unsteady phenomena will be less pronounced than in the systems where the same diameters are used. It is possible that this is the case in actual systems where additional damping of pressure waves occurs at the connections between pipes with different diameters. In the conducted studies, local damping at the "Y" junction was not considered, so it seems that the additional damping resulting from the interference of primary and secondary waves forming at the "Y" junction is the cause of this phenomenon.

4 Conclusions

This paper investigated a number of emergency shutdowns of a hydraulic system consisting of reservoirs, valves, and pipes. In single-pipe Systems 1 and 2, where the flow occurred between two reservoirs, the pressure calculated by the Joukowsky formula was not exceeded. In a more complex system comprised of three reservoirs that are connected by a Y-shaped pipe junction, the situation can be much more severe. It turns out that as a result of wave interference, maximum and minimum pressures (despite security measures transient vaporous cavitation occurred in few tests) in these systems can be significantly higher and lower, respectively. The objective of this paper is to draw attention to this engineering problem and to encourage analysts to perform extensive numerical transient tests of newly designed pipe networks to reduce failure risks early in the design stage (pipe leaks, ruptures of hydraulic components, etc.).

All tests were conducted using a freeware computer code Allievi, which excels in: efficient calculation time; a number of applicable boundary conditions; simple user-friendly design environment; free license, etc. At this time the code does not consider the frequency-dependent skin friction (based on a convolution integral, which is the only theoretically verified method) and retarded strain effects (that are responsible for damping and dissipation of pressure waves during unsteady flows in plastic pipes). In few simulations steady flow convergence problems occurred (inaccurate calculation of initial flow velocities).

Further verification of the obtained computational results for a much longer simulation time are planned in the near future (observation of possible resonance effects). It is planned to use in-house written software that takes into account unsteady friction and viscoelasticity of plastic pipes. Numerical results will be compared with the results of measurements performed in a new pipeline apparatus and to results from new analytical solutions (for laminar flow only).



Appendix A Tables with Quantitative Results

Table 3 Quantitative results of Damping Ratio Coefficient *DRC* for Systems 1 and 2

Pipe material	Type of flow	$Wh = 0.0001$ $D = 4$ cm (Water flow)		$Wh = 0.001$ $D = 12.5$ cm (Water-oil emulsion flow)		$Wh = 0.01$ $D = 30$ cm (Oil flow)	
		N3 valve 1	N7 valve 2	N3 valve 1	N7 valve 2	N3 valve 1	N7 valve 2
		System 1					
steel pipe	laminar	0.9999	–	0.9967	–	0.9586	–
	transitional	0.9995	–	0.9914	–	0.9367	–
	turbulent	0.9983	–	0.9791	–	0.9146	–
PVC pipe	laminar	0.9999	–	0.9918	–	0.9681	–
	transitional	0.9996	–	0.9884	–	0.9469	–
	turbulent	0.9979	–	0.9750	–	0.9201	–
System 2							
steel pipe	laminar	0.9998	0.9999	0.9981	0.9981	0.9706	0.9850
	transitional	0.9995	0.9998	0.9952	0.9952	0.9598	0.9697
	turbulent	0.9986	0.9993	0.9877	0.9874	0.9348	0.9541
PVC pipe	laminar	0.9998	0.9999	0.9981	0.9981	0.9396	0.9568
	transitional	0.9997	0.9998	0.9968	0.9967	0.9675	0.9728
	turbulent	0.9986	0.9991	0.9896	0.9893	0.9396	0.9568



Table 4 Quantitative results of Over Pressure Coefficient OPC for System 3

Test	Flow type	OPC [-]		
		L_1 pipe	L_2 pipe	L_3 pipe
$D = \text{const} = 4 \text{ cm}$				
3.1.1	laminar	1.00	1.00	1.00
3.1.2	laminar	2.00	2.80	3.46
3.1.3	laminar	1.80	2.57	3.64
3.1.4	laminar	1.68	2.72	5.73
3.1.5	turbulent	0.99	1.00	1.00
3.1.6	turbulent	1.89	3.07	3.30
3.1.7	turbulent	1.80	2.59	3.62
3.1.8	turbulent	1.70	2.87	4.35
$Re = \text{const}$				
3.2.1	laminar	1.91	1.69	1.53
3.2.2	laminar	2.22	2.41	2.12
3.2.3	laminar	2.73	2.34	2.11
3.2.4	laminar	2.42	2.41	2.46
3.2.5	transitional	1.88	1.72	1.44
3.2.6	transitional	2.19	2.44	2.06
3.2.7	transitional	2.72	2.33	2.08
3.2.8	transitional	2.42	2.41	2.46
3.2.9	turbulent	1.81	1.80	1.32
3.2.10	turbulent	2.18	2.57	1.81
3.2.11	turbulent	2.42	2.34	2.23
3.2.12	turbulent	2.60	2.25	2.32

Appendix B Large Scale Three-Reservoir-Pipe System

Table 5 Pipe lengths, calculated pressure heads and velocities

Test	Flow type	L_1 [m]	L_2 [m]	L_3 [m]	v_1 [m/s]	v_2 [m/s]	v_3 [m/s]	H_{R1} [m]	H_{R2} [m]	H_{R3} [m]
$D = \text{const} = 60 \text{ cm}$										
3.1.9	turbulent	1000	300	100	0.1833	0.1100	0.0733	34.629	34.572	34.577

The appendix will discuss a case (Test 3.1.9) that is similar to cases presented in the main body of the paper but for large values of Reynolds numbers occurring in pipes with a relatively large diameter $D=0.6$ m (15 times larger than for Test 3.1.8). The data are shown in Table 5. It follows that pipe lengths are 20 times longer than that for Test 3.1.8. The Reynolds numbers are: $Re_1=100000$; $Re_2=60000$; $Re_3=40000$ (ten times higher than for Test 3.1.8). The pressure wave speed calculated in Allievi is 1304.44 m/s.

Comparison of the results for Test 3.1.8 with those obtained for Test 3.1.9 reveals a noticeable similarity of the obtained pressure pulsation waveforms (Fig. 4 versus Fig. 7). The pressure at the N5 node ("Y" junction) is in phase opposite to the pulsations occurring at the nodes of the L_1 conduit, i.e. N3 and N4. In the L_2 and L_3 conduits, the pressures at the nodes N6 and N7 as well as at N10 and N11 occur in the same phase.



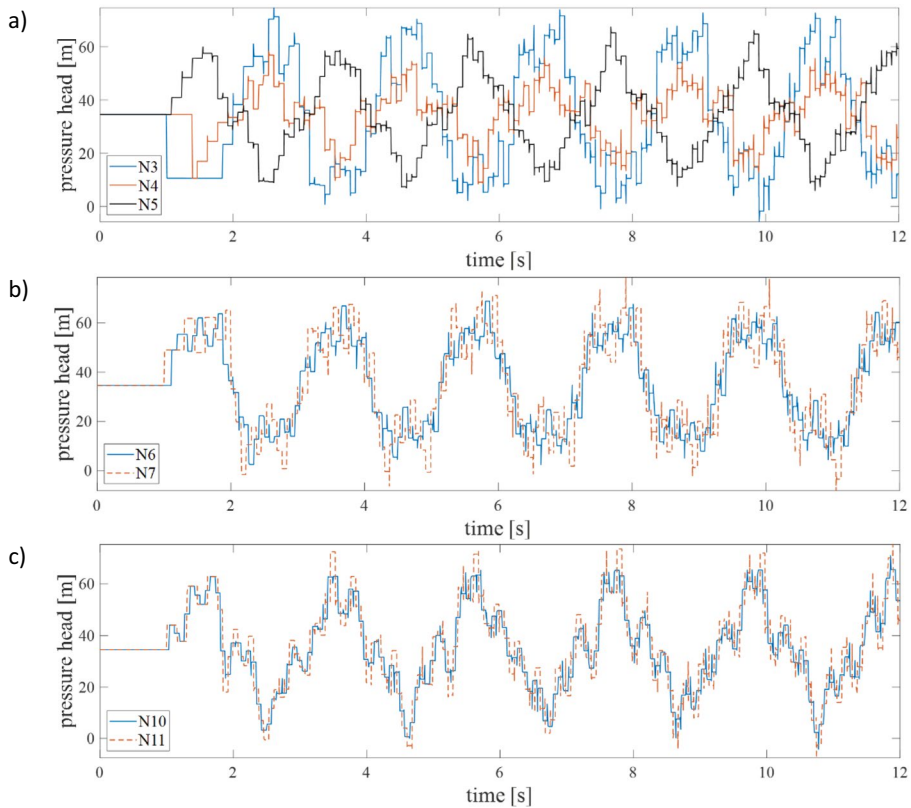


Fig. 7 Results for turbulent flow case in the large scale three-reservoir system (Test 3.1.9; $L_1=1000$ m, $L_2=300$ m and $L_3=100$ m)

The maximum pressures in the respective pipes are at the same nodes: L_1 (node N3), L_2 (node N7), and L_3 (node N11). A qualitatively noticeable similarity is proved by quantitative research too. The following values of *OPC* quantitative parameters were obtained: L_1 pipe – *OPC* = 1.66; L_2 pipe – *OPC* = 3.04 and L_3 pipe – *OPC* = 4.28. The obtained results are therefore very close to those obtained for Test 3.1.8 (see Table 4). This indicates that the most important factor for the analyzed wave interaction are the length ratios (L_2 / L_1 and L_3 / L_1) of the designed pipe system.

Author Contributions [KU]: Conceptualization, Methodology, Validation, Writing – original draft, Supervision. [IH]: Formal analysis, Software, Investigation. [AB]: Conceptualization, Software, Formal analysis, Writing – original draft. [AD]: Investigation, Resources, Project administration.

[PŚ]: Visualization, Data curation, Software, Funding acquisition.

Availability of Data and Materials Data supporting the findings of this study are available from the corresponding author [KU] on request.

Declarations

Ethical Approval Not applicable.



Consent to Participate Not applicable.

Consent to Publish Not applicable.

Competing Interests The authors have no relevant financial or non-financial interests to disclose.

Open Access This article is licensed under a Creative Commons Attribution 4.0 International License, which permits use, sharing, adaptation, distribution and reproduction in any medium or format, as long as you give appropriate credit to the original author(s) and the source, provide a link to the Creative Commons licence, and indicate if changes were made. The images or other third party material in this article are included in the article's Creative Commons licence, unless indicated otherwise in a credit line to the material. If material is not included in the article's Creative Commons licence and your intended use is not permitted by statutory regulation or exceeds the permitted use, you will need to obtain permission directly from the copyright holder. To view a copy of this licence, visit <http://creativecommons.org/licenses/by/4.0/>.





References

- Allievi Homepage (n.d.) <https://www.allievi.net/allievi-es.php>. Last accessed 05 May 2023
- Andrade DM et al (2022) A new model for fluid transients in piping systems taking into account the fluid–structure interaction. *J Fluids Struct* 114:103720
- Andrade DM et al (2023) Fluid transients in viscoelastic pipes via an internal variable constitutive theory. *Appl Math Model* 114:846–869
- Bayle A, Plouraboué F (2023) Spectral properties of fluid structure interaction pressure/stress waves in liquid filled pipes. *Wave Motion* 116:103081
- Bergant A et al (2010) Water hammer and column separation due to accidental simultaneous closure of control valves in a large-scale two-phase flow experimental test rig. In: Proceedings of the ASME 2010 Pressure Vessels & Piping Division / K-PVP Conference PVP2010, July 18–22. Bellevue, Washington, USA, paper: PVP2010–26131, pp 923–932
- Bergant A et al (2021) Developments in multiple-valve water-hammer control. *IOP Conf Ser Earth Environ Sci* 774(1):012008
- Bostan M et al (2021) An implicit approach for numerical simulation of water hammer induced pressure in a straight pipe. *Water Resour Manag* 35:5155–5167
- Cao Z et al (2022) Unsteady friction model modified with compression–expansion effects in transient pipe flow. *AQUA - Water Infrastruct Ecosyst Soc* 71(2):330–344
- Capponi C et al (2023) Hydraulic diagnostic kit for the automatic expeditious survey of in-line valve sealing in long, large diameter transmission mains. *Water Resour Manag* 37:1931–1945
- Haidera MA, Valentine EM (2018) An effective alternate method for solving the classic three reservoirs and multi-reservoirs problem. *Civil Eng Res Mag (CERM)* 40(3):129–140
- Han Y et al (2022) Effects of closing times and laws on water hammer in a ball valve pipeline. *Water* 14(9):1497
- Karadžić U et al (2018) Water hammer and column separation induced by simultaneous and delayed closure of two valves. *J Mechl Eng* 64(9):525–535
- Kim SH (2023) Generalized impedance-based transient analysis for multi-branched pipeline systems. *Water Resour Manag* 37:1581–1597
- Kodura A (2016) An analysis of the impact of valve closure time on the course of water hammer. *Arch Hydro-Eng Environ Mech* 63(1):35–45
- Liao J, Li B (2010) Research on coupled water hammer in hydraulic pipe system. *Appl Mech Mater* 29–32:401–406
- Loganathan GV, Kuo CY (1985) A direct solution for the classical three reservoir problem. *Civ Eng Pract Des Eng* 4:1–11
- Lončar G et al (2019) Numerical models for analysis of hydraulic transients. *Int Symp Water Manag Hydraul Eng, WMHE, Skopje, North Macedonia* 05–07.09:133–145
- Lupa SI et al (2022) Investigation of water hammer overpressure in the hydraulic passages of hydropower plants equipped with Francis turbines. *IOP Conf Ser Earth Environ Sci* 1079:012003
- Pan B et al (2022) Transient energy analysis in water-filled viscoelastic pipelines. *J Hydraul Eng* 148(1):04021051

- Ramoul S et al (2017) Numerical modeling of transient flows in load pipes with complex geometry. *J Appl Math Comput Mech* 16(4):67–78
- Rangaraju KG, Sathuraman S (1969) Direct solution of three-reservoir problem. *Civil Eng J* 11(3–4):15–23
- Singh R (1982) Direct solution of three-reservoir problem. *J Inst Eng (India): Civil Eng Div* 62(5):292–296
- Sun X et al (2017) Transient flow analysis of integrated valve opening process. *Nucl Eng Des* 313:296–305
- Swamee DK, Jain AK (1972) Explicit equations for pipe flow problems. *J Hydraul Div* 102:657–664
- Taieb LH et al (2020) Effect of integrating polymeric pipes on the pressure evolution and failure assessment in cast iron branched networks. *Eng Fract Mech* 235:107158
- Tijsseling AS, Bergant A (2012) Exact computation of waterhammer in a three-reservoir system. In: Anderson S (ed) *BHR Group Proc. of the 11th Int. Conf. Pressure Surges*. pp 161–170
- Urbanowicz K (2017) Computational compliance criteria in water hammer modelling. *E3S Web Conf* 19:03021
- Urbanowicz K et al (2023) Developments in analytical wall shear stress modelling for water hammer phenomena. *J Sound Vib* 562:117848
- Wang X et al (2019) Effect of multi-valve closure on superposed pressure in a tree-type long distance gravitational water supply system. *J Water Supply Res Technol AQUA* 68(6):420–430
- Wylie EB et al (1993) *Fluid transients in systems*. Prentice-Hall Inc., Englewood Cliffs, New Jersey
- Yuce MI, Omer AF (2019) Hydraulic transients in pipelines due to various valve closure schemes. *SN Appl Sci* 1:1110
- Zhang Q et al (2023) Numerical simulation of water hammer in pipeline system using efficient wave tracking method. *Water Resour Manag* 37:3053–3068
- Zhang ZH (2016) Transient flows in a pipe system with pump shut-down and the simultaneous closing of a spherical valve. *IOP Conf Ser Earth Environ Sci* 49:052001

Publisher's Note Springer Nature remains neutral with regard to jurisdictional claims in published maps and institutional affiliations.

Authors and Affiliations

Kamil Urbanowicz¹  · Igor Haluch¹ · Anton Bergant²  · Adam Deptuła³  ·
Paweł Śliwiński⁴ 

✉ Kamil Urbanowicz
kamil.urbanowicz@zut.edu.pl

Igor Haluch
haluchigor@gmail.com

Anton Bergant
anton.bergant@litostrojpower.eu

Adam Deptuła
a.deptula@po.edu.pl

Paweł Śliwiński
pawel.sliwinski@pg.edu.pl

- ¹ Faculty of Mechanical Engineering and Mechatronics, West Pomeranian University of Technology in Szczecin, Szczecin, Poland
- ² Faculty of Mechanical Engineering, Litostroj Power d.o.o. (Full-Time) and University of Ljubljana (Part-Time), Ljubljana, Slovenia
- ³ Faculty of Production Engineering and Logistics, Opole University of Technology, Opole, Poland
- ⁴ Faculty of Mechanical Engineering and Ship Technology, Gdansk University of Technology, Gdańsk, Poland

